Materials Transactions, Vol. 43, No. 9 (2002) pp. 2181 to 2184

Magnetic Properties of Ni–Mn Alloys with Dispersed Ferromagnetic Nanoparticles *1

Teiko Okazaki, Yositaka Kumeta *2 and Yasuo Sakisaka

Faculty of Science and Technology, Hirosaki Unversity, Hirosaki 036-8561, Japan

We investigated the magnetic properties of $Ni_{1-x}Mn_x$ ($x = 0.20$–0.30) alloys with dispersed nanoparticles having a ferromagnetic Ni_3Mn ordered phase, which is caused by suitable heat treatment. Magnetic analysis shows that for $0.3 \geqq x > 0.25$ alloys interaction between 4–10 nm particles through Mn-rich matrix is antiferromagnetic. The Néel temperature increases with both Mn concentration and long-range-order parameter. On the contrary, for $0.25 > x \geqq 0.20$ alloys, interaction between $\sim$4 nm particles through Ni-rich matrix is ferromagnetic. These alloys exhibit soft magnetic properties and have permeability of 400–600 for 1–500 kHz high frequency.

(Received April 24, 2002; Accepted July 4, 2002)

Keywords: *$Ni_{1-x}Mn_x$ ($x = 0.20$–0.30) alloy, ferromagnetic ordered phase, nanoparticle, Néel temperature, soft magnetic property*

1. Introduction

In Ni_3Mn alloy system, a Cu_3Au-type ordered phase is formed after suitable heat treatment. A change in the degree of the long-range order causes a wide variety of the magnetic and transport properties.[1,2] The Ni_3Mn alloy annealed at 693 K has ferromagnetic nanoparticles dispersed in disordered paramagnetic matrix and shows giant magnetoresistance (GMR).[3,4]

In previous study, as seen in Fig. 1,[5] we have observed that GMR occurs in nanoparticle inhomogeneous $Ni_{1-x}Mn_x$ ($x = 0.20$–0.30) alloys and found that the GMR depends remarkably on Mn concentration. For $x < 0.25$ alloys, the MR ratio from -0.5% to -1.0% consists of GMR and anisotropic behavior which arises from a ferromagnetic phase (Type I). On the contrary, the GMR for $x > 0.25$ alloys increases steeply with annealing time and reaches a maximum of -3.6% for $Ni_{0.73}Mn_{0.27}$ alloy of 693 K·100 h state (Type II).

In this study, we investigate the origin of different behavior of GMR with Mn concentration to be clear. Furthermore, we report soft magnetic properties of $Ni_{1-x}Mn_x$ ($x = 0.20$–0.25) alloys having nanocrystalline structures.

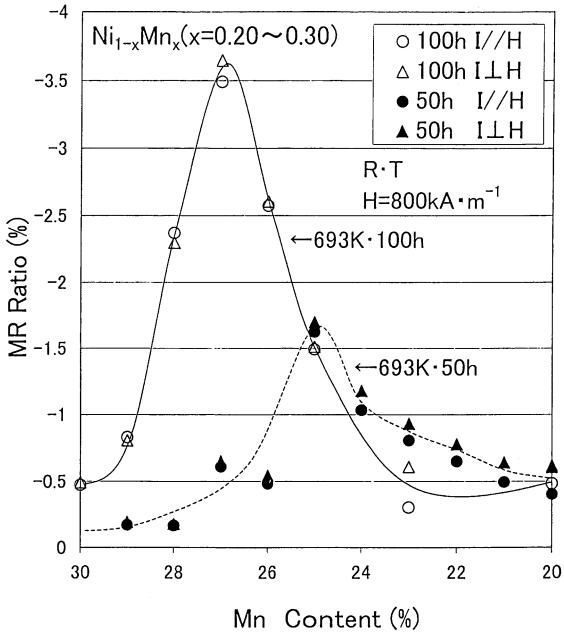

Fig. 1 Dependence of MR ratio ($\Delta\rho/\rho_0 \parallel H$ and $\perp H$) for $Ni_{1-x}Mn_x$ ($x = 0.20$–0.30) at room temperature on Mn concentration.

2. Experimental Procedure

Sample preparation procedures of $Ni_{1-x}Mn_x$ ($x = 0.20$, 0.23, 0.26, 0.27, 0.28, 0.29, 0.30) alloys were previously reported.[3] Each alloy, melted in an rf induction furnace, was shaped into a ribbon (5.0 mm in width, 0.45 mm in thickness) and a wire ($\phi = 0.5$ mm). Some of wires were annealed for 10 h at 1273 K in order to get homogeneous alloy. They were annealed in Ar for various hours at 673 K, 693 K and 713 K to get ordered states.

The X-ray diffraction (XRD) of ribbon samples was taken with Cu Kα radiation. The long-range-order parameter S was determined by comparing the integral intensity of the (110) peak caused by super-lattice formation to that of the (220) peak. The loop of magnetization M vs. magnetic field H was measured with a vibrating sample magnetometer. Permeability of wire specimen for 1–500 kHz high frequency was measured by impedance analyzer.

3. Results and Discussion

3.1 Long-range-order parameter *S*, average particle size *D* and lattice constant

Long-range-order parameter S, average particle size D and lattice constant for ribbon samples annealed for 100 h and 200 h at 693 K are listed in Table 1. S increases from 0.3 to 0.76 with Mn concentration and changes a little with annealing time from 100 h to 200 h. The value of D was determined from the broadening of the XRD (110) peak of the ordered phase by using Scherrer's equation. D increases from about

*1 This Paper was Presented at the Spring Meeting of the Japan Institute of Metals, held in Tokyo, on March 30, 2002.

*2 Graduate Student, Hirosaki University.

Table 1 The lattice constant a, the long-range-order parameter S, average cluster size D and the volume fraction of the ordered regions $\varepsilon = S^2/S_{do}^2$ for $Ni_{1-x}Mn_x$ alloys ($x = 0.20$–0.30).

	693 K·100 h				693 K·200 h		
x	a/nm	S	D/nm	ε	S	D/nm	ε
0.20	0.3576	0.28	~4	0.08			
0.23	0.3586	0.39	6	0.15			
0.24	0.3587	0.44	4.6	0.19			
0.26	0.3590	0.66	4.3	0.44	0.66	6.8	0.44
0.27	0.3593	0.7	5.1	0.49	0.74	6.6	0.55
0.28	0.3600	0.66	6.5	0.44	0.76	9.9	0.58
0.29	0.3601	0.72	6.1	0.52	0.68	5.2	0.46
0.30	0.3603	0.67	6.7	0.45	0.75	7.5	0.55

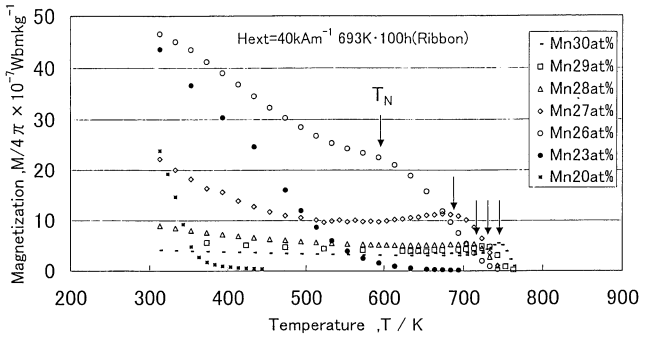

Fig. 2 Magnetization vs. temperature curves of $Ni_{1-x}Mn_x$ ($x = 0.20$, 0.23, 0.26, 0.27, 0.28, 0.29, 0.30) ribbons annealed for 100 h at 693 K.

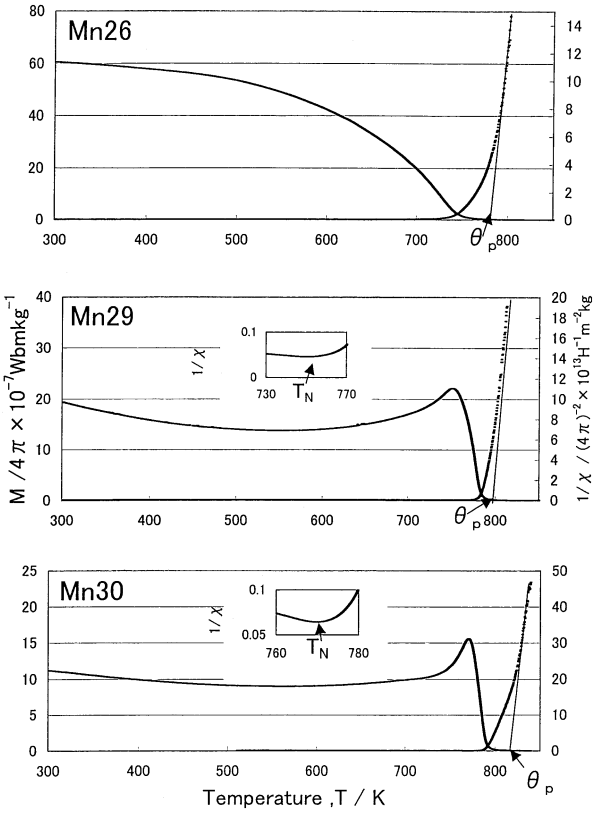

Fig. 3 Magnetization vs. temperature and the inverse susceptibility $1/\chi$-T curves of $Ni_{1-x}Mn_x$ ($x = 0.26$, 0.29, 0.30) ribbons annealed for 200 h at 693 K.

4 to 10 nm with both x and annealing time. The volume fraction ε in the nano-scale ordered regions (*i.e.*, nanoparticles) can be evaluated by the relationship,[6] $\varepsilon = S^2/S_{do}^2$, where S_{do} is the long-range-order parameter in the ordered domains. Assuming $S_{do} = 1$, ε is about 0.1 to 0.6 for $S = 0.3$ to 0.76 states. ε is nearly constant value of 0.5 for $Ni_{1-x}Mn_x$ alloys of $0.26 \leqq x \leqq 0.30$. The lattice constant also increases with x. The phenomenon is caused by increase of antiferromagnetic Mn–Mn pairs with x. The Mn–Mn distance (0.264 nm)[7] is longer than the ferromagnetic Ni–Mn (0.253 nm)[7] and Ni–Ni (0.249 nm) distances.

3.2 Dependence of Néel temperature on Mn concentration

Figures 2 and 3 show the magnetization M vs. temperature T curves of $Ni_{1-x}Mn_x$ ($x = 0.20$, 0.23, 0.26, 0.27, 0.28, 0.29, 0.30) ribbons annealed for 100 h and 200 h at 693 K, respectively.

In Fig. 2, it is found that magnetic feature in inhomogeneous phase of these alloys are quite different.

The magnetization of applied field 40 kA m^{-1} at 300 K decreases from 47 to $4 \times 4\pi \times 10^{-7}$ Wb m kg^{-1} with Mn concentration. Moreover, each M-T curve for alloys of $x = 0.26$, 0.27, 0.28, 0.29 and 0.30 has a cusp (as denoted by arrows) in temperature range of 700 K $< T <$ 750 K which grows with x, but alloys of $x = 0.20$ and 0.23 do not have a cusp and therefore are ferromagnetic (Curie temperature T_F is 344 K and 511 K determined by Arrott plot, respectively).

Figure 3 shows both the M-T and the inverse susceptibility $1/\chi$-T curves for alloys of $x = 0.26$, 0.29 and 0.30 at applied field of 80 kA m^{-1}. Each $1/\chi$-T curve has a minimum at 732 K, 750 K and 770 K for $x = 0.28$, 0.29 and 0.30, respectively. The minimum corresponds to a Néel temperature T_N, where antiferromagnetic coupling between nanoparticles disappears. While, there is no minimum in $1/\chi$-T curve of $Ni_{0.74}Mn_{0.26}$. The paramagnetic Curie point θ_P of each alloy determined from $1/\chi$-T relation is given in Fig. 4. As shown in Fig. 4, T_N and θ_P increase with annealing time except T_N of alloys of $x = 0.26$ and 0.27, where the situations are ambiguous.

3.3 Magnetic phase and interaction between nanoparticles mediated by matrix

Figure 4 exhibits magnetic phase and Mn-concentration dependence of T_F, T_N, θ_P and order-disorder transition temperature T_C,[8] where F, A·F, S·P and P mean ferromagnetic, antiferromagnetic, super-paramagnetic and paramagnetic phases, respectively. T_C of $Ni_{1-x}Mn_x$ ($x = 0.20$–0.30) alloy increases from 710 to 850 K with x. $\theta_{P\,200\,h}$ also increases from 775 to 805 K with increasing x from 0.26 to 0.30. $\theta_{P\,200\,h}$ is just below T_C, where ferromagnetic Ni_3Mn ordered phase translates to disordered paramagnetic one. Moreover, there is also $T_{N\,200\,h}$ in temperature range of 30–70 K just below T_C.

We think that interaction between nanoparticles is mediated by disordered matrix. The magnetism of Ni_3Mn depends on the number of the nearest-neighbor Mn atoms around a Mn atom,[9] because a ferromagntic interaction operates for the Ni–Ni and Ni–Mn pairs and an antiferromagnetic one for Mn–Mn pairs. In previous papers,[4] we reported that the inho-

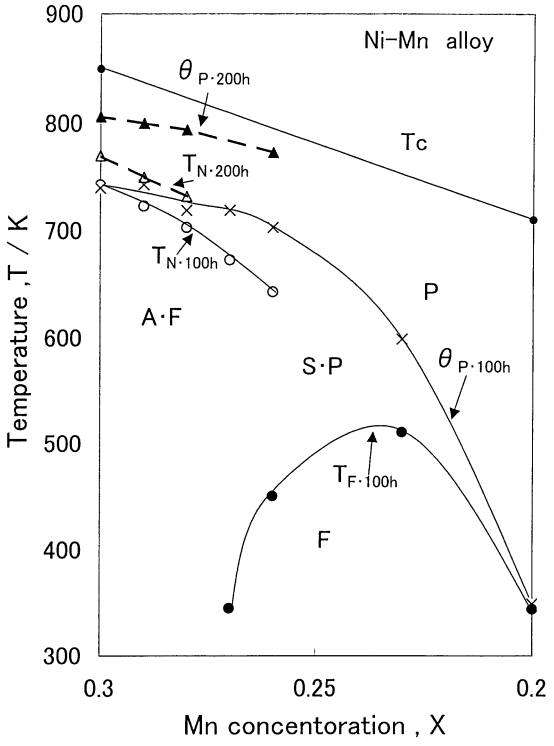

Fig. 4 Magnetic phase and Mn-concentration dependence of T_F, T_N, θ_P and order-disorder transition temperature T_C. There, F, A·F, S·P and P mean ferromagnetic, anti-ferromagnetic, super-paramagnetic and paramagnetic phases, respectively.

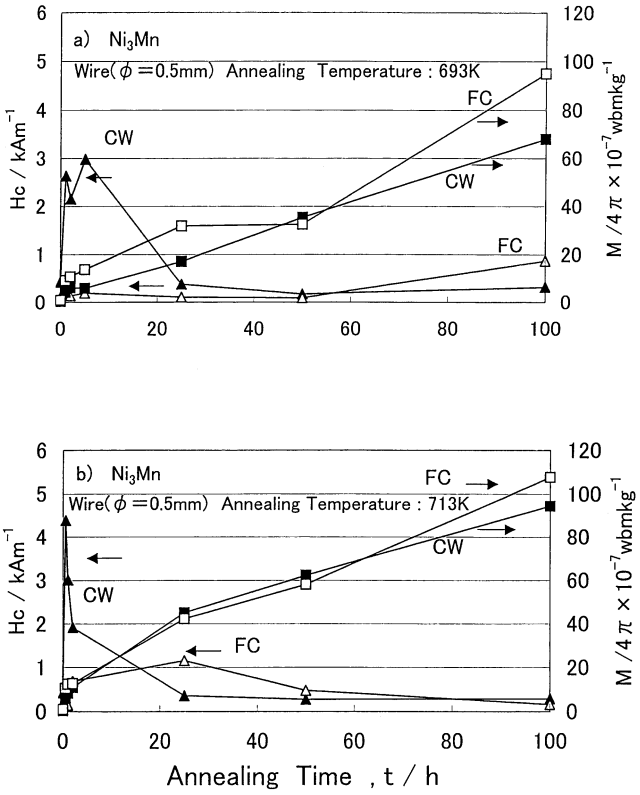

Fig. 5 Annealing-time dependence of the coercive force H_C and saturation magnetization M_S for Ni_3Mn wire sample at (a) 693 K and (b) 713 K. There, FC and CW denote furnace cool and cold-working of wire.

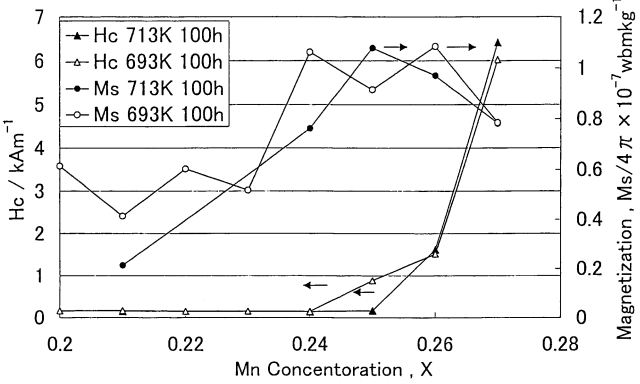

Fig. 6 Mn-concentration dependence of H_C ($H_{ext} = 40\,kA\,m^{-1}$) and M_S ($H_{ext} = 400\,kA\,m^{-1}$) of wires annealed for 100 h at 693 K and 713 K.

mogeneous $Ni_{0.75}Mn_{0.25}$ alloy annealed at 693 K consists of nano-scale ordered domains (*i.e.*, nanoparticles) distributed in disordered paramagnetic matrix (the average exchange coupling around a Mn atom, $J_{ex} \sim 0$), where GMR in granular ferromagnetic systems arises. The present alloys with Mn concentration of $x < 0.25$ or $x > 0.25$ have Ni-rich ($J_{ex} > 0$) or Mn-rich ($J_{ex} < 0$) matrices, respectively, after super-lattice Ni_3Mn nanoparticles are precipitated.

From the results of the magnetic phase and the volume fraction of nanoparticles, it is thought that matrix of Type I arisen in GMR (see Fig. 1) is characterized with ferromagnetic coupling due to Ni–Ni pairs and matrix of Type II with antiferromagnetic coupling due to Mn–Mn pairs. The strength of antiferromagnetic coupling increases with size of nanoparticle. The T_F of their ordered phase raises up as more complete super-lattice is formed with longer annealing time.

3.4 Soft magnetic property

Nano-scale inhomogeneous Ni_3Mn alloy has soft magnetic properties where the particles couple to each other ferromagenetically.[10] That is, the saturation magnetic flux density increases but the coercive force decreases with the ferromagnetic particle size.

Figure 5 shows the dependency of the coercive force H_C and saturation magnetization M_S for Ni_3Mn wire sample on annealing time t at 693 K and 713 K. There, FC and CW denote furnace cool and cold-working of wire. M increases with t for all samples and reaches to a maximum 68–108 $\times$ $4\pi \times 10^{-7}\,Wb\,m\,kg^{-1}$ at $t = 100$ h. M_S for Ni_3Mn of $S \sim 1$ was obtained to be $108 \times 4\pi \times 10^{-7}\,Wb\,m\,kg^{-1}$.[10]

While the H_C increases in the initial ordered state, especially for CW sample, and then decreases slowly to 0.18–0.3 kAm^{-1} except one for FC 693 K·100 h state. Very similar behavior was also seen in the ribbon samples.[10]

Figure 6 shows the dependency of H_C ($H_{ext} = 40\,kA\,m^{-1}$) and M_S ($H_{ext} = 400\,kA\,m^{-1}$) of wires annealed for 100 h at 693 K and 713 K on Mn concentration. Both values depend on x remarkably. The value of H_C is small and equal to about $0.2\,kA\,m^{-1}$ for wire of $0.20 \leqq x \leqq 0.24$, but it increases with $x > 0.25$. It is considered that the wire of $0.24 \leqq x \leqq 0.26$ annealed at 693 K consists of nanoparticle being almost ordered state of $S = 1$.

From the results, soft magnetic property due to the nanocrystalline morphology is expected to occur in wire of $x < 0.26$.

Figure 7 shows 1–500 kHz high frequency permeability of

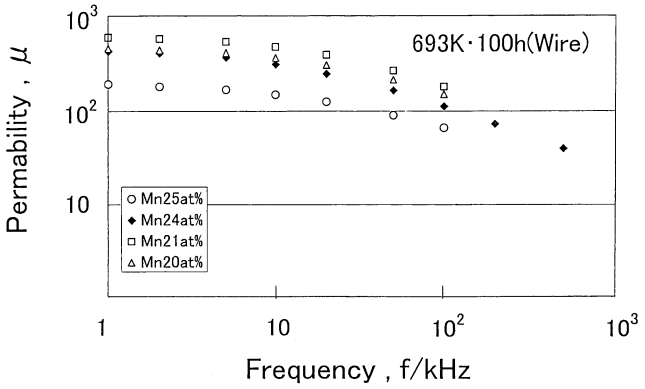

Fig. 7 High frequency permeability of $Ni_{1-x}Mn_x$ ($x = 0.20$, 0.21, 0.24, 0.25) wires annealed for 100 h at 693 K.

$x = 0.20$, 0.21, 0.24, 0.25 wires annealed for 100 h at 693 K. The permeability for $f = 1$–20 kHz is high, 200–600, but decreases slowly for $f > 20$ kHz, because of loss due to eddy currents. To overcome this limitations, it should be necessary to prepare and study fiber or foil samples.

4. Conclusion

We investigated the magnetic properties of $Ni_{1-x}Mn_x$ ($x = 0.20$–0.30) alloys with dispersed ferromagnetic nanoparticles ordered by heat-treatment. The main conclusions are as follows:

(1) The values of long-range-order parameter, average particle size and volume fraction of ordered phase are 0.3–0.76, 4–10 nm and 0.1–0.6, respectively, and increase with Mn concentration.

(2) $Ni_{1-x}Mn_x$ alloy of $x \leqq 0.26$ has ferromagnetic, superparamagneic and paramagnetic phases, while the alloy of $x \geqq 0.26$ has antiferromagnetic and paramagnetic phases.

(3) The nanoparticles are coupled ferromagenetically mediated by ferromagenetic Ni-rich matrix for alloy of $x \leqq 0.24$ and antiferromagetically by antiferromagenetic Mn-rich matrix for $x \geqq 0.26$.

(4) $Ni_{1-x}Mn_x$ alloys of $x \leqq 0.24$ exhibit soft magnetic property and have permeability of 400–600 for 1–500 kHz high frequency.

Acknowledgements

The authors are grateful to Professors S. Mitani and K. Yamada for experimental help and valuable discussion.

REFERENCES

1) S. Kaya and M. Nakayama: Proc. Phys.-Math. Soc. Jpn. **22** (1940) 126–141.
2) M. J. Marcinkowski and N. Brown: J. Appl. Phys. **32** (1961) 375–386.
3) T. Okazaki and Y. Kondo: Mater. Trans., JIM **39** (1998) 231–236.
4) T. Okazaki, S. Sugimoto, Y. Aono, T. Miyanaga and M. Homma: Jpn. J. Appl. Phys. **38** (1999) 5071–5074.
5) T. Okazaki, T. Miyanaga, K. Sawaguchi, Y. Sakisaka and S. Sugimoto: J. M. M. M. **239** (2002) 189–191.
6) A. Paoletti, F. P. Ricci and L. Passari: J. Appl. Phys. **37** (1966) 3236–3239.
7) A. V. Ryazhkin, Yu. A. Babanov, V. P. Pilugin, T. Miyanaga, T. Okazaki, E. D. Crozier and R. A. Gordon: J. Synchrotron Rad. **8** (2002) 300–301.
8) M. Hansen: *Constitution of Binary Alloys*, (McGraw-Hill, New York, 1958).
9) T. Okazaki: Jpn. J. Appl. Phys. **34** (1995) 1537–1541.
10) T. Okazaki, K. Sawaguchi and M. Homma: Mater. Trans., JIM **41** (2000) 1150–1153.